



# Combined automated 3D volumetry by pulmonary CT angiography and echocardiography for detection of pulmonary hypertension

Claudius Melzig<sup>1,2</sup> · Stefan Wörz<sup>3</sup> · Benjamin Egenlauf<sup>4</sup> · Sasan Partovi<sup>5</sup> · Karl Rohr<sup>3</sup> · Ekkehard Grünig<sup>2,4</sup> · Hans-Ulrich Kauczor<sup>1,2</sup> · Claus Peter Heussel<sup>1,2,6</sup> · Fabian Rengier<sup>1,2,7</sup> 

Received: 26 December 2018 / Revised: 13 February 2019 / Accepted: 20 March 2019 / Published online: 8 April 2019  
© European Society of Radiology 2019

## Abstract

**Objectives** To assess the diagnostic accuracy of automated 3D volumetry of central pulmonary arteries using computed tomography pulmonary angiography (CTPA) for suspected pulmonary hypertension alone and in combination with echocardiography. **Methods** This retrospective diagnostic accuracy study included 70 patients (mean age 66.7, 48 female) assessed for pulmonary hypertension by CTPA and transthoracic echocardiography with estimation of the pulmonary arterial systolic pressure (PASP). Gold standard right heart catheterisation with measurement of the invasive mean pulmonary arterial pressure (invasive mPAP) served as the reference. Volumes of the main, right and left pulmonary arteries (MPA, RPA and LPA) were computed using automated 3D segmentation. For comparison, axial dimensions were manually measured. A linear regression model was established for prediction of mPAP (predicted mPAP).

**Results** MPA, RPA and LPA volumes were significantly increased in patients with vs. without pulmonary hypertension (all  $p < 0.001$ ). Of all measures, MPA volume demonstrated the strongest correlation with invasive mPAP ( $r = 0.76, p < 0.001$ ). Predicted mPAP using MPA volume and echocardiographic PASP as covariates showed excellent correlation with invasive mPAP ( $r = 0.89, p < 0.001$ ). Area under the curves for predicting pulmonary hypertension were 0.94 for predicted mPAP, compared to 0.90 for MPA volume and 0.92 for echocardiographic PASP alone. A predicted mPAP  $> 25.8$  mmHg identified pulmonary hypertension with sensitivity, specificity, positive and negative predictive values of 86%, 93%, 95% and 81%, respectively.

**Conclusions** Automated 3D volumetry of central pulmonary arteries based on CTPA may be used in conjunction with echocardiographic pressure estimates to noninvasively predict mPAP and pulmonary hypertension as confirmed by gold standard right heart catheterisation with higher diagnostic accuracy than either test alone.

## Key Points

- *This diagnostic accuracy study derived a regression model for noninvasive prediction of invasively measured mean pulmonary arterial pressure as assessed by gold standard right heart catheterisation.*
- *This regression model using automated 3D volumetry of the central pulmonary arteries based on CT pulmonary angiography in conjunction with the echocardiographic pressure estimate predicted pulmonary arterial pressure and the presence of pulmonary hypertension with good diagnostic accuracy.*
- *The combination of automated 3D volumetry and echocardiographic pressure estimate in the regression model provided superior diagnostic accuracy compared to each parameter alone.*

**Keywords** Pulmonary arteries · Pulmonary artery volumetry · Pulmonary artery pressure · Pulmonary hypertension · Computed tomography angiography

✉ Fabian Rengier  
fabian.rengier@web.de

Extended author information available on the last page of the article

## Abbreviations

CT	Computed tomography
CTPA	Computed tomography pulmonary angiography
LPA	Left pulmonary artery
MPA	Main pulmonary artery
mPAP	Mean pulmonary arterial pressure
mPAP <sub>predicted</sub>	mPAP predicted by linear regression
mPAP <sub>RHC</sub>	mPAP measured by right heart catheterisation
MRI	Magnetic resonance imaging
PASP	Transthoracic echocardiographic pulmonary arterial systolic pressure estimate
PH	Pulmonary hypertension
RHC	Right heart catheterisation
RPA	Right pulmonary artery

## Introduction

Pulmonary hypertension (PH) is a chronic condition defined by an elevation of the mean pulmonary arterial pressure (mPAP)  $\geq 25$  mmHg at rest measured by right heart catheterisation (RHC) [1]. PH can occur primarily or as a consequence of a variety of diseases including left heart disease, lung disease and chronic thromboembolic disease [2]. If left untreated, PH carries a poor prognosis with persistent elevation of pulmonary arterial pressure leading to irreversible remodelling of the pulmonary vasculature and eventually right heart failure [3, 4]. Thus, early diagnosis and therapeutic intervention are crucial to improve outcome. However, clinical symptoms of PH like dyspnoea, fatigue and palpitations are non-specific and often do not immediately suggest the diagnosis of PH [1]. Furthermore, RHC as an invasive procedure is ultimately required to establish the diagnosis, but might be delayed due to its potential complications [5].

Functional imaging like echocardiography and magnetic resonance imaging (MRI) has been investigated for noninvasive diagnosis of PH [6–9]. The drawbacks of echocardiographic measurements of pulmonary arterial systolic pressure (PASP) are its high variability and observer-dependence, and MRI is limited by its low availability and high cost [10]. Computed tomography (CT), on the other hand, is frequently clinically indicated and performed in patients with suspected PH to rule out other causes for the presenting symptoms such as pulmonary embolism or parenchymal lung disease. Thus, it appears a promising approach to use these routinely acquired CT data for the detection of PH.

Although increased diameters of the central pulmonary arteries have been repeatedly shown to indicate PH and can be reliably identified by CT, literature suggests variable diagnostic accuracy for the detection of PH with particular limitations regarding the sensitivity and negative predictive value [11–16]. Subsequent studies presented analyses of 3D

pulmonary artery geometry and indicated better agreement with PH compared with pulmonary artery diameters [17–21]. However, these studies were limited by their study design as case-control studies and further relevant methodological shortcomings, especially selection bias with cases being limited to a single subgroup of PH and controls being healthy subjects or subjects without suspicion of PH, or the lack of gold standard RHC. Thus, diagnostic accuracy of 3D pulmonary artery dimensional measures in a consecutive patient cohort with suspected PH against the gold standard RHC has not been performed yet to our knowledge.

The purpose of this study was to assess diagnostic accuracy of automated 3D volumetry of the central pulmonary arteries based on CT pulmonary angiography (CTPA) against RHC as the gold standard in patients with suspected PH and to establish whether a combination of this technique and echocardiographic measurements yields higher diagnostic accuracy than either test alone.

## Materials and methods

### Patients

This retrospective study was approved by the institutional review board. Informed consent requirement was waived because of its retrospective nature. Records of all patients undergoing RHC, CTPA and transthoracic echocardiography for the initial diagnostic workup of suspected pulmonary hypertension in our institution between August 2013 and June 2015 were retrospectively reviewed ( $n = 94$ ). Exclusion criteria were signs of chronic thromboembolic disease on CTPA ( $n = 13$ ), an interval between CTPA and RHC of more than 30 days ( $n = 3$ ), non-diagnostic CTPA ( $n = 3$ ), missing RHC measurements ( $n = 1$ ) or missing echocardiographic PASP measurements ( $n = 4$ ) resulting in a final study population of  $n = 70$  (Table 1). Signs of chronic thromboembolic disease on CTPA was chosen as an exclusion criterion because intraluminal thrombi can be expected to decrease the contrast-enhanced vessel lumen thereby resulting in falsely low vessel volume measurements. Patient characteristics (gender, height, weight, age) were extracted from the records; body surface area was calculated according to the formula by Du Bois and Du Bois [22].

### CTPA acquisition

All CTPA data were acquired as part of the diagnostic workup of suspected PH using a clinical CT scanner (Somatom Definition AS64, Siemens Healthineers). All CTPA scans were performed in a supine position in inspiratory breath-hold. Scanning parameters were as follows: automated tube voltage selection and tube current modulation (CareDose 4D,

**Table 1** Clinical characteristics of the study population

	No PH	PH	<i>p</i> value
Number of subjects	27	43	–
Female	22 (81.5%)	26 (60.5%)	0.07
Age (years)	59.2 ± 14.7	71.4 ± 8.0	<0.001
Body surface area (m <sup>2</sup> )	1.82 ± 0.21	1.85 ± 0.23	0.62
mPAP <sub>RHC</sub> (mmHg)	16.7 ± 3.6	37.8 ± 10.9	<0.001
Systolic PAP <sub>RHC</sub> (mmHg)	26.0 ± 5.7	60.8 ± 20.6	<0.001
Diastolic PAP <sub>RHC</sub> (mmHg)	10.7 ± 2.9	24.7 ± 7.1	<0.001
PAWP <sub>RHC</sub> (mmHg)	8.9 ± 3.4	14.6 ± 7.7	<0.001
PVR <sub>RHC</sub> (dyn × s × cm <sup>-5</sup> )	125.9 ± 45.6	418.7 ± 265.5	<0.001
PASP (mmHg)	30.3 ± 6.5	56.6 ± 19.8	<0.001
WHO classification			
Group 1	–	18 (42%)	–
Group 2	–	16 (37%)	–
Group 3	–	9 (21%)	–
Group 5	–	0	–

Data is given as mean ± SD, % or *n*, respectively. *PH*, pulmonary hypertension; *RHC*, right heart catheterisation; *mPAP<sub>RHC</sub>*, mean pulmonary arterial pressure; *systolic PAP<sub>RHC</sub>*, systolic pulmonary arterial pressure; *diastolic PAP<sub>RHC</sub>*, diastolic pulmonary arterial pressure; *PAWP<sub>RHC</sub>*, pulmonary arterial wedge pressure; *PVR<sub>RHC</sub>*, pulmonary vascular resistance; *PASP*, transthoracic echocardiographic pulmonary arterial systolic pressure estimate. Groups were compared using two-sided Student's *t* test or Pearson's chi-squared test as appropriate

Siemens Healthineers), bolus tracking in the main pulmonary artery, 50 ml of iodinated contrast agent (Ultravist 300, Bayer HealthCare) followed by a saline bolus of 50 ml, iterative reconstruction kernel I40f level 3 and reconstructed slice thickness of 1 mm with 0.7 mm increment.

## Echocardiography

Transthoracic echocardiography was performed using a modern echocardiography system (Vivid E95, GE Healthcare). Echocardiographic PASP estimates were obtained applying the standard protocol used internationally across centres [23, 24]. In short, the pressure gradient between the right atrium and right ventricle is estimated by measuring the velocity of a tricuspid regurgitation jet using the modified Bernoulli equation. Diameter and collapsibility of the inferior vena cava serve as estimators for the right atrial pressure. Summation of the estimated pressure gradient and the estimated right atrial pressure results in the echocardiographic PASP estimate.

## Right heart catheterisation

RHC was performed according to standard procedures [1] by two interventional pneumologists each with more than 5 years of experience in RHC. In short, an 8 French introducer sheath was placed in the right internal jugular vein under ultrasound guidance after local anaesthetics. A 7 French pulmonary artery catheter (Swan-Ganz thermodilution catheter 7F 110 cm, Edwards Lifesciences) was placed into the main pulmonary artery for the measurement of mean pulmonary arterial

pressure by RHC (mPAP<sub>RHC</sub>). Zero levelling of the pressure transducer was done at the mid-thoracic line according to international guidelines [1]. Pulmonary arterial pressure was recorded in the main pulmonary artery above the pulmonary valve. Measurements were recorded and assessed using MacLab and CardioSoft (both GE Healthcare). The interventional pneumologists had access to the clinical information and to the results of the echocardiography, but not to the results of the 3D segmentation of CTPA data as described below.

## Image analysis

After anonymisation of all CT data sets, analysis was performed in random order and blinded to any clinical data including RHC measurements. Automated 3D segmentation was performed using an in-house developed model-based segmentation software. The respective algorithms have been previously published and validated in detail [25–27]. Inter- and intraobserver agreements of the algorithm were assessed in a previous study with excellent intraclass correlation coefficients of 0.995–0.999 for the main, right and left pulmonary arteries [17]. In short, after manual placement of seeding points, the software fits a three-dimensional analytical intensity model to the voxel intensity values within a region of interest thereby creating a three-dimensional model of the respective vessel. The model fit is then further improved by applying an automatic two-step refinement procedure. The segmentation process is completed within seconds.

Automated segmentation was performed for main (MPA), right (RPA) and left (LPA) pulmonary arteries in a standardised manner. First, seeding points were placed in each of the pulmonary arteries to start the segmentation process. The reader then verified the segmentation process and manually defined each vessel segment by marking the level of the pulmonary valve, the main pulmonary artery bifurcation as well as the branch-off point of right and left upper lobe pulmonary arteries (Fig. 1). The software then calculated vessel volume and vessel length of each pulmonary artery. The volume of each pulmonary artery (MPA, RPA and LPA) was then indexed for its respective vessel length and corrected for the subject's body surface area: MPA volume, RPA volume and LPA volume.

For comparison with current clinical routine, axial diameters of MPA, RPA, LPA and ascending aorta were manually measured at standardised locations as described previously [17]: MPA and ascending aortic diameters were obtained at the level of the RPA as described in the Framingham Heart Study [28]. RPA and LPA diameter were each measured 1.5 cm distally to the MPA bifurcation. The ratio of the MPA diameter to the ascending aorta diameter was calculated. All axial measurements were performed in a randomised order and blinded to the diagnosis and the results of the 3D segmentation. All image analyses were performed by a radiologist with 4 years of experience in cardiovascular imaging.

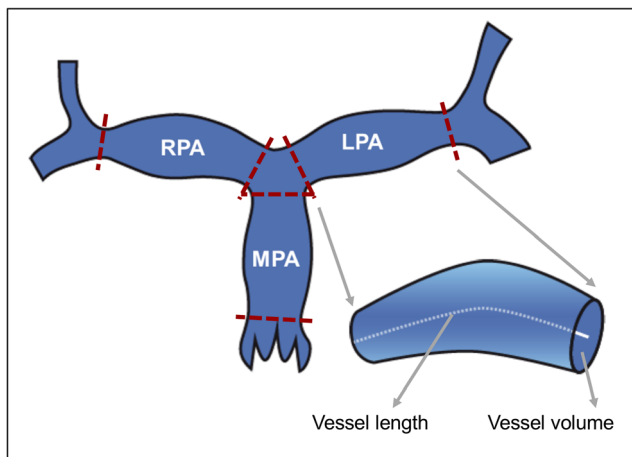


**Fig. 1** The segmentation process. The volumes of the main, right and left pulmonary arteries (MPA, RPA and LPA, respectively) are defined by the levels of the pulmonary valve, the MPA bifurcation and the branch-off point of the respective upper lobe artery

### Statistical analysis

Data for statistical analysis was complete with the exception of RPA volume of 1 patient (1.4% of patients) and LPA volumes of 3 patients (4.3% of patients) because segmentation was technically not successful in these cases. Little's test was used to verify missingness completely at random ( $p > 0.05$ ). Expectation maximisation method was then used to impute the missing values for RPA volume and LPA volume. Expectation maximisation imputation was performed based on all complete volume measurements before correction for BSA. Normal distribution of measurements was tested and confirmed using the Kolmogorov-Smirnov test. Correlation between pulmonary artery volumes, axial dimensions and  $mPAP_{RHC}$  was analysed using Pearson's correlation. Comparison between patients with PH and patients without PH was performed by two-sided Student's  $t$  tests. Gender distribution was compared using Pearson's chi-squared test. A forward stepwise multivariate linear regression analysis was performed to derive a numerical model for noninvasive  $mPAP$  prediction ( $mPAP_{predicted}$ ) using axial dimensions, pulmonary artery volumetry and echocardiographic PASP as covariates with a required variable significance of 0.05 to be included into the model, and a cut-off value of 0.1 for exclusion. Receiver operating characteristic (ROC) analyses were performed and areas under the curve were calculated to assess the diagnostic performance to detect PH by means of axial dimensions, pulmonary artery volumetry and echocardiographic PASP as well as the linear regression model for  $mPAP_{predicted}$  integrating these variables as covariates. Sensitivities, specificities as well as positive and negative predictive values were calculated.  $p$  values  $< 0.05$  were considered statistically significant. All statistical analyses were performed using SPSS Version 24.0 (SPSS Inc.).

The sample size was estimated based on the dedicated software Power Analysis and Sample Size applying the procedure Tests for One-Sample Sensitivity and Specificity which uses the methodology by Li and Fine (PASS 11, NCSS, LLC) [29, 30]. Calculation was made using the following prerequisites and assumptions: alpha level 0.05, power 0.8, prevalence of disease among the study population 50%, null hypothesis sensitivity and specificity 70% and alternative hypothesis sensitivity and specificity 90%. The calculated sample size was 62 patients including a minimum of 31 patients with pulmonary hypertension.

## Results

### Study cohort

Mean age of the study cohort was  $66.7 \pm 12.5$  years, age range 19–84 years. 48 (68.6%) of the 70 included patients were female. Forty-three patients (61%) were diagnosed with PH on RHC ( $mPAP_{RHC} \geq 25$  mmHg), 27 patients (39%) had normal pulmonary arterial pressures on RHC. Further patient characteristics are summarised in Table 1.

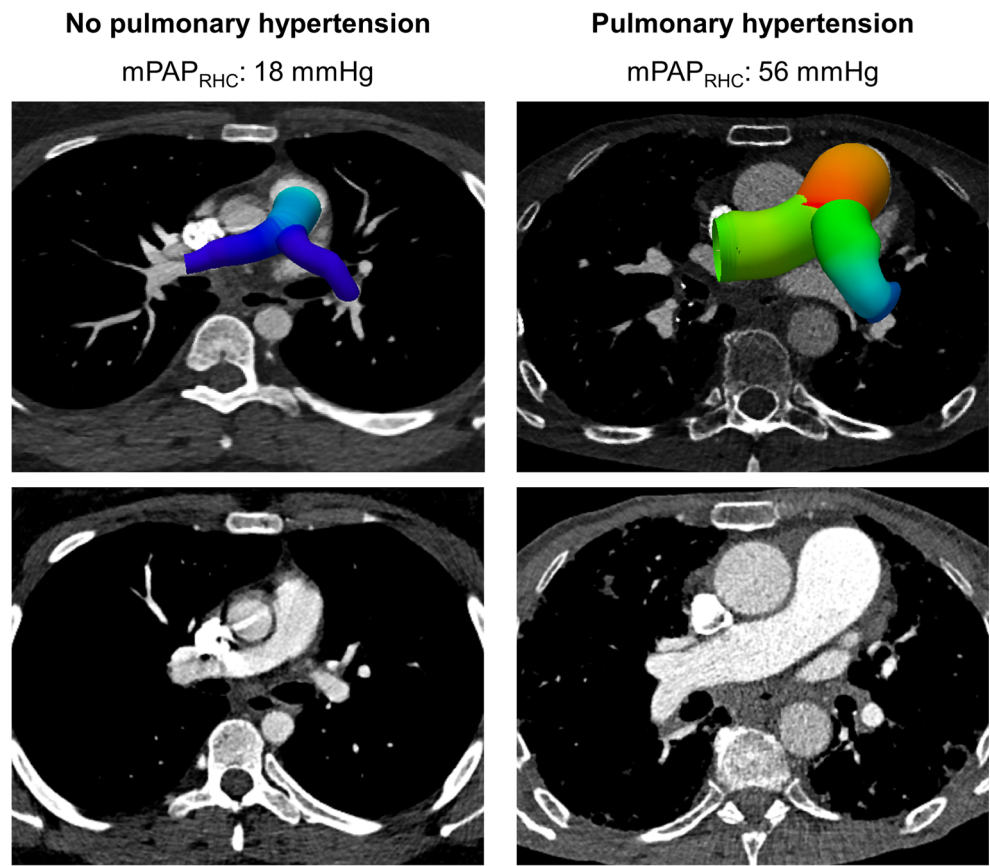
### Axial dimensions

Mean axial diameters of MPA, RPA and LPA in millimetres were  $33.1 \pm 5.1$ ,  $28.5 \pm 5.0$  and  $27.1 \pm 4.6$  in patients with PH compared to  $24.6 \pm 4.1$ ,  $21.3 \pm 4.8$  and  $21.6 \pm 5.2$  in patients without PH (all  $p < 0.001$ ). MPA to ascending aorta diameter ratio was  $0.92 \pm 0.14$  in patients with PH compared to  $0.73 \pm 0.09$  in patients without PH ( $p < 0.001$ ). Correlation of axial dimensions with  $mPAP_{RHC}$  was good for MPA with a correlation coefficient of  $r = 0.68$  or  $r^2 = 0.46$  ( $p < 0.001$ ) and for MPA to ascending aorta diameter ratio with  $r = 0.68$  or  $r^2 = 0.46$  ( $p < 0.001$ ), and moderate for RPA with  $r = 0.53$  or  $r^2 = 0.28$  ( $p < 0.001$ ) and for LPA with  $r = 0.47$  or  $r^2 = 0.22$  ( $p < 0.001$ ).

### Pulmonary artery volumes

Segmentation was successful in 98.1% of cases (Fig. 2). RPA in 1 patient (1.4% of patients) and LPA in 3 patients (4.3% of patients) could not be successfully segmented. All these cases were due to imaging artefacts (motion and beam hardening artefacts due to influx of contrast media via the superior vena cava) which misled automated segmentation to include out-of-vessel structures. Mean MPA volume, RPA volume and LPA volume in  $\mu\text{l}/(\text{mm} \times \text{m}^2)$  were  $490.5 \pm 121.2$ ,  $343.6 \pm 107.6$  and  $308.0 \pm 78.2$  in patients with PH compared to  $287.7 \pm 90.3$ ,  $193.6 \pm 77.6$  and  $216.7 \pm 92.2$  in patients without PH (all  $p < 0.001$ , Fig. 3). There was no significant difference between female and male patients in MPA volume ( $404.8 \pm 153.2$  vs.  $428.4 \pm 137.8$ ,  $p > 0.52$ ), RPA volume ( $276.5 \pm$

**Fig. 2** Representative examples of automated 3D segmentation results of the central pulmonary arteries in a patient without pulmonary hypertension (left) and in a patient with severe pulmonary hypertension (right). Colour-coding visualises vessel size. Axial slices of the same patients are shown in the lower row



124.3 vs. 306.0 ± 114.9,  $p > 0.34$ ) and LPA volume (264.8 ± 100.6 vs. 290.1 ± 78.9,  $p > 0.26$ ).

MPA volume showed a strong correlation with  $mPAP_{RHC}$  with a correlation coefficient of  $r = 0.73$  or  $r^2 = 0.53$

( $p < 0.001$ , Fig. 4). RPA volume and LPA volume demonstrated moderate to good correlation with  $mPAP_{RHC}$  (Fig. 4). To avoid multicollinearity, regression analyses were therefore based on MPA volume.

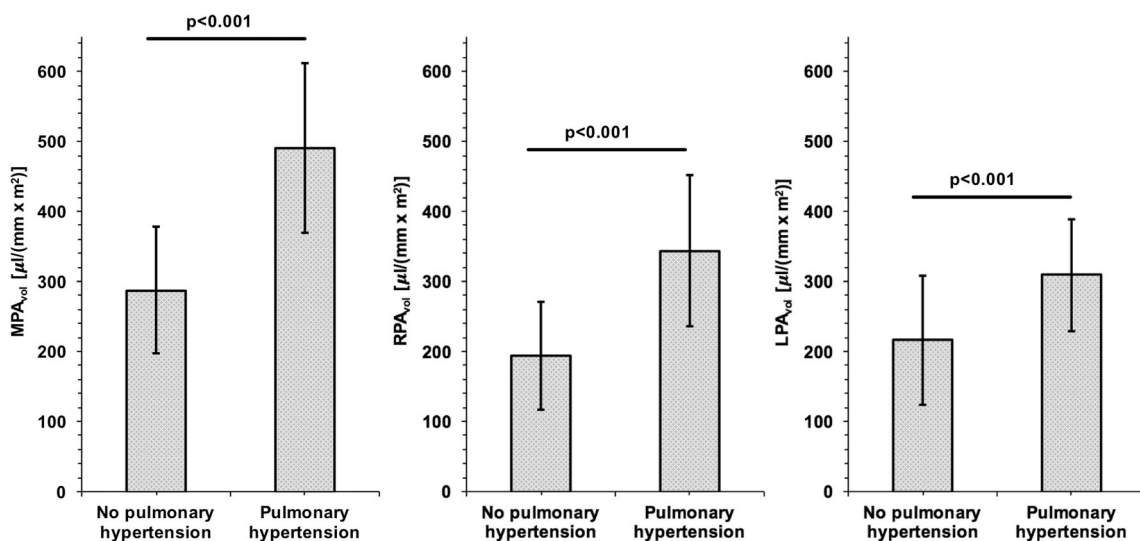


**Fig. 3** Bar charts of CTPA-derived vessel volumes of the main, right and left pulmonary arteries (MPA volume, RPA volume and LPA volume, respectively) for patients without and with pulmonary hypertension

according to the gold standard right heart catheterisation illustrating significant enlarged pulmonary artery volumes in patients with pulmonary hypertension as analysed by two-sided Student's *t* tests

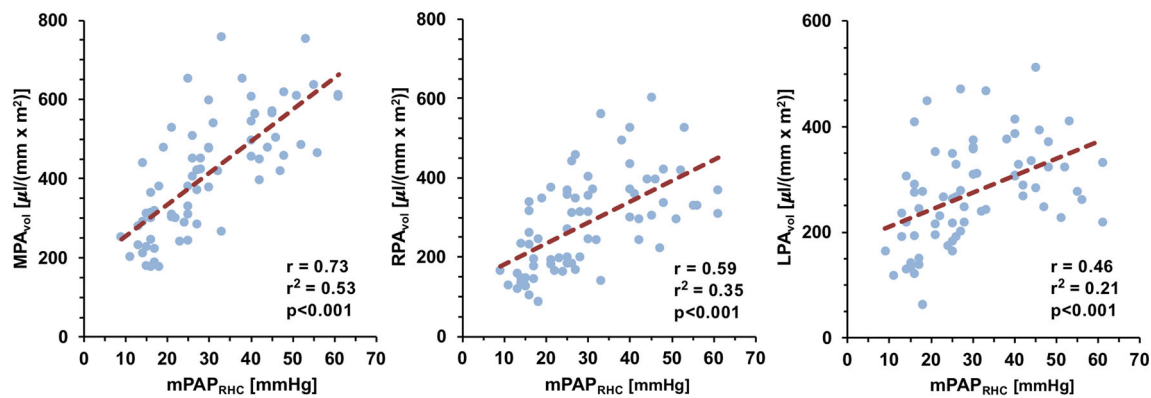


**Fig. 4** Scatter plots for CTPA-derived volumes of the main, right and left pulmonary arteries (MPA volume, RPA volume and LPA volume, respectively) and  $mPAP_{RHC}$  illustrating a significant correlation

between noninvasively measured volumes and invasively measured  $mPAP_{RHC}$  as assessed by Pearson's correlation. Dashed lines indicate linear regression fit

### Noninvasive estimation of pulmonary hypertension

The stepwise multivariate linear regression showed the best diagnostic accuracy when including MPA volume assessed by CTPA and echocardiographic PASP as covariates and excluding axial diameter of MPA. The following model for noninvasive prediction of  $mPAP_{RHC}$  was determined:  $mPAP_{predicted} = 0.029 \times \text{MPA volume} + 0.438 \times \text{echocardiographic PASP} - 2.635$  ( $r = 0.89/r^2 = 0.80$ ,  $p < 0.001$ , Fig. 5). Standardised beta-coefficients for MPA volume and echocardiographic PASP were 0.32 and 0.66, respectively.

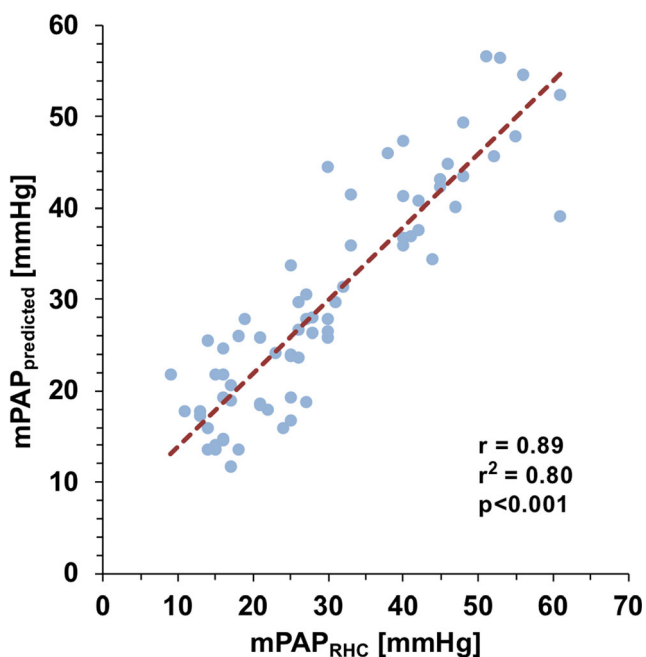


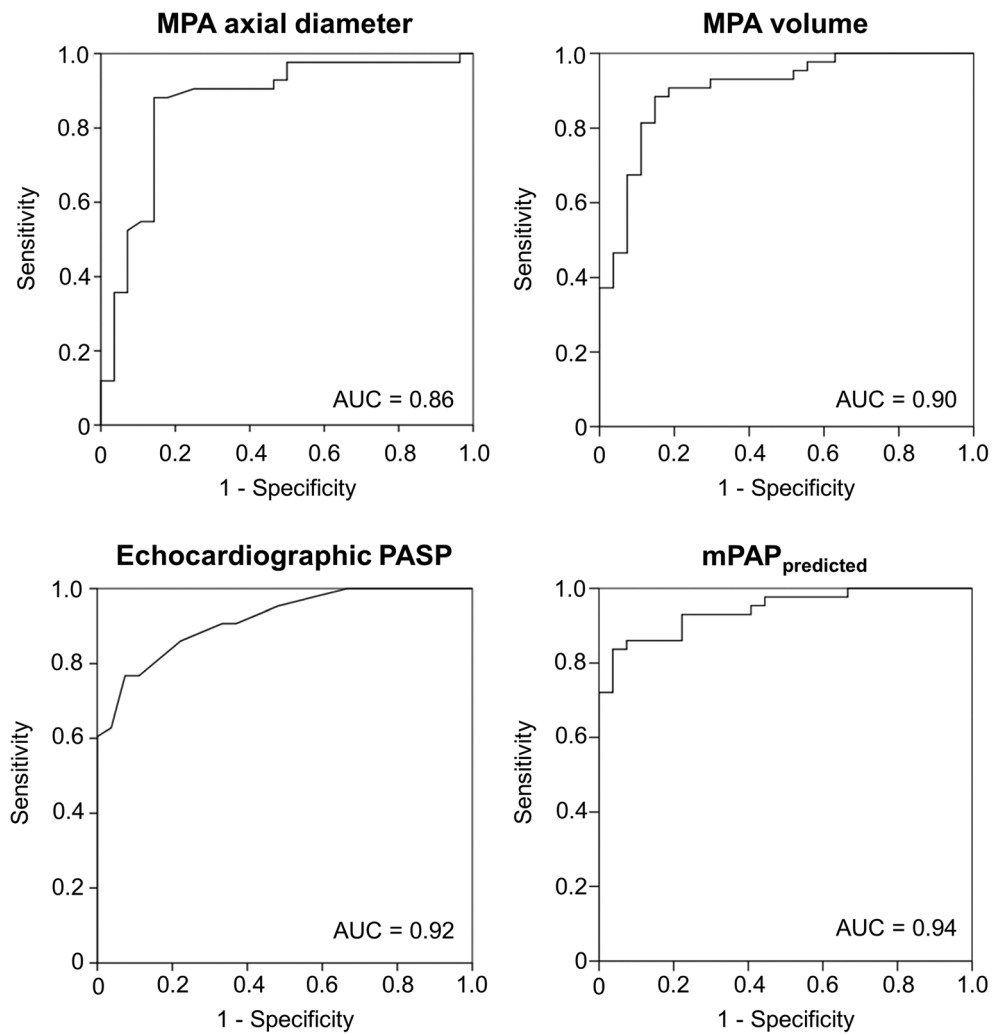
**Fig. 5** Scatter plot for noninvasive  $mPAP_{predicted}$  and invasive  $mPAP_{RHC}$ .  $mPAP_{predicted}$  was calculated after establishing a linear regression model with CTPA-derived MPA volume and echocardiographic PASP as covariates. Dashed line indicates linear regression fit

ROC analysis demonstrated areas under the curve of 0.94 for  $mPAP_{predicted}$  (95% CI 0.89–0.99,  $p < 0.001$ ) compared to 0.86 for axial diameter of MPA (95% CI 0.77–0.96,  $p < 0.001$ ), 0.90 for MPA volume alone (95% CI 0.83–0.98,  $p < 0.001$ ) and 0.92 for echocardiographic PASP alone (95% CI 0.86–0.98,  $p < 0.001$ ) (Fig. 6). Applying the same cut-off value of  $\geq 25$  mmHg as in gold standard RHC, sensitivity, specificity, positive and negative predictive values of  $mPAP_{predicted}$  for predicting the presence of PH were 86% (95% CI 72.1–94.7%), 85% (95% CI 66.3–95.8%), 90% (95% CI 78.8–95.8%) and 79% (95% CI 64.2–89.1%), respectively, with a Youden index of 0.71. Using a cut-off value of  $\geq 25.8$  mmHg resulted in the maximum diagnostic accuracy with a Youden index of 0.79 and sensitivity, specificity, positive and negative predictive values of 86% (95% CI 72.1–94.7%), 93% (95% CI 75.7–99.1%), 95% (95% CI 82.9–98.6%) and 81% (95% CI 66.3–89.8%), respectively (Table 2). For comparison, axial diameter of MPA had lower diagnostic accuracy with sensitivity, specificity, positive and negative predictive values of 79% (95% CI 64.0–90.0%), 89% (95% CI 70.8–97.7%), 92% (95% CI 79.4–97.1%) and 73% (95% CI 59.5–82.9%), respectively, using a cut-off value of  $> 29$  mm. For MPA volume alone, sensitivity, specificity, positive and negative predictive values were 88% (95% CI 74.9–96.1%), 85% (95% CI 66.3–95.8%), 91% (95% CI 79.3–95.9%) and 82% (95% CI 66.5–91.4%), respectively.

### Discussion

This study derived a regression model for noninvasive prediction of  $mPAP_{RHC}$  and the presence of PH using automated 3D volumetry of the central pulmonary arteries based on CTPA and echocardiographic PASP measurements. The regression model was compared against gold standard RHC and showed good diagnostic accuracy. The combination of MPA volume

**Fig. 6** Receiver operating characteristic curves for the detection of pulmonary hypertension. Areas under the curves are given for each technique: MPA axial diameter and MPA volume based on CTPA, echocardiographic PASP and linear regression model ( $mPAP_{\text{predicted}}$ ) as described in the text



and echocardiographic PASP in the regression model provided superior diagnostic accuracy compared to each parameter alone. Automated 3D volumetry also demonstrated significantly enlarged volumes of the main, right and left pulmonary arteries in patients with PH compared with patients without PH. The technique of 3D volumetry provided robust quantitative results in the great majority of cases.

**Table 2** Diagnostic accuracy of noninvasive prediction of invasively measured  $mPAP$

	$mPAP_{RHC}$		Sum
	< 25 mmHg	≥ 25 mmHg	
$mPAP_{\text{predicted}}^* < 25.8$ mmHg	25	6	31
$mPAP_{\text{predicted}}^* \geq 25.8$ mmHg	2	37	39
Sum	27	43	70

\* $mPAP_{RHC}$ : mean pulmonary arterial pressure; *RHC*, right heart catheterisation. Indicates that the cut-off value is based on the maximum Youden index

Noninvasive prediction of PH based on CTPA appears to be a promising approach for translation into clinical routine. CTPA is performed in many of the patients with suspected PH either as part of the diagnostic workup for the presenting symptoms even before PH is suspected or as part of the diagnostic algorithm for suspected PH. Previous studies about CTPA in PH focused on measurements of pulmonary artery diameters and pulmonary artery to aorta diameter ratio [11, 14–16, 31, 32]. These studies yielded variable results regarding diagnostic accuracy for the detection of PH with particular limitations regarding the sensitivity and negative predictive value. In our study, MPA axial diameter showed good correlation with  $mPAP_{RHC}$  with a correlation coefficient of  $r = 0.68$  and an area under the curve of 0.86 for the detection of PH. Nonetheless, MPA volume was superior with a stronger correlation coefficient of  $r = 0.73$  with  $mPAP_{RHC}$  and an area under the curve of 0.90.

This advantage of 3D volumetry over diameter measurements is well in accordance with previous studies [17–19]. One case-control study with 41 participants based on MRI

demonstrated improved identification of patients with known pulmonary arterial hypertension, i.e. group 1 PH according to the World Health Organisation classification, by 3D volume measurements compared to diameter measurements of the central pulmonary arteries, but did not evaluate diagnostic accuracy against the gold standard RHC [17]. Another case-control study with 16 participants with chronic sleep apnoea syndrome reported high correlation between intrapulmonary vessel volume and mPAP measured by RHC, but was limited by study design and lacked comparison with diameter measurements [18]. The potential of 3D volumetry has also been described for other vascular systems, for example in the setting of abdominal aortic aneurysms [33, 34]. This advantage of 3D volumetry may be due to the more accurate detection of morphologic changes in all three dimensions and the higher reliability of a three-dimensional measurement as opposed to a one-dimensional-diameter measurement [17].

Our study showed an improvement of diagnostic accuracy for detecting PH when combining CTPA-derived pulmonary artery volumes with echocardiographic pressure estimates with a significant contribution of both individual measures. This is consistent with previous studies showing higher diagnostic accuracy when combining pulmonary artery diameter measurements with echocardiographic pressure estimates [35, 36]. The individual, incremental value of these measurements can be explained by the complementary nature of morphological parameters like 3D volumes and functional parameters like echocardiographic PASP estimates. Since echocardiography is also routinely performed for the investigation of PH, echocardiographic PASP values are available for practically all patients with suspected PH. Although echocardiography alone is used for noninvasive prediction of pulmonary arterial pressures in current clinical practice, the inherent limitations of echocardiography like the required degree of expertise and dependency on adequate imaging conditions lead to substantial variability of measurements [10]. The areas under the curve of 0.92 of echocardiographic PASP for diagnosing PH in our study is comparably high and within the upper range reported in the literature, but is found to be lower in most studies [8].

First of all, we believe that even a relatively small improvement of a noninvasive diagnostic test as demonstrated in this study is particularly clinically relevant when an invasive diagnostic test, i.e. RHC, could potentially be avoided. Certainly, this has to be investigated in future prospective studies. Second, we believe that investigation of 3D volumetry techniques is important from a scientific point of view even at this early stage of clinical research both for advancing knowledge and prompting further research irrespective of its current clinical relevance. Principally, the 3D volumetry technique could be well integrated into the clinical workflow. We used an in-house-developed solution, but commercially available processing tools for centreline analysis provide similar functionalities with equal fast segmentation, excellent repeatability and minimal user interaction [37, 38].

This study is subject to some limitations. First, the retrospective study design may have introduced a selection bias. Nevertheless, the patient cohort of our study closely resembles the patient population that might benefit most of the investigated 3D volumetry technique, namely patients with suspected PH of any cause. Second, it may be criticised that patients with chronic thromboembolic PH were secondarily excluded. This exclusion criterion was defined because intraluminal thrombi can be expected to decrease the contrast-enhanced vessel lumen and thus result in falsely low vessel volume quantification. Since the present study revealed MPA volume as the measure with the strongest correlation with  $mPAP_{RHC}$  and chronic thromboemboli very rarely affect the MPA itself, future studies should include patients with chronic thromboembolic disease. Another point of criticism might be that the group without PH had a lower mean age compared with the group with PH. However, younger subjects tend to have larger pulmonary arteries thereby potentially decreasing rather than increasing the contribution of 3D volume measures in the linear regression model [28]. In addition, the body surface area was very similar for patients with and without PH. Finally, evaluation of inter- and intraobserver agreement did not form part of our present study because our previous study demonstrated excellent inter- and intraobserver agreement with intraclass correlation coefficients of 0.995–0.999 for MPA, RPA and LPA [17].

In conclusion, automated 3D volumetry of the central pulmonary arteries based on CTPA may be used in conjunction with transthoracic echocardiographic PASP measurements to noninvasively estimate mPAP and predict PH as confirmed by gold standard RHC with higher diagnostic accuracy than either test in isolation. Prospective studies are warranted to verify the value of the presented technique in the diagnostic workup of patients with suspected PH.

**Funding** This study was supported by the German Center for Lung Research (DZL) through grants from the German Ministry for Education and Science (BMBF; 82DZL00401, 82DZL00402, 82DZL00404).

## Compliance with ethical standards

**Guarantor** The scientific guarantor of this publication is Fabian Rengier.

**Conflict of interest** The authors of this manuscript declare no relationships with any companies whose products or services may be related to the subject matter of the article.

**Statistics and biometry** One of the authors has significant statistical expertise.

**Informed consent** Written informed consent was waived by the Institutional Review Board.



**Ethical approval** Institutional Review Board approval was obtained.

### Methodology

- retrospective
- diagnostic or prognostic study
- performed at one institution

### References

- Galiè N, Humbert M, Vachieri J-L et al (2015) 2015 ESC/ERS guidelines for the diagnosis and treatment of pulmonary hypertension. *Eur Heart J* 37:67–119
- Simonneau G, Gatzoulis MA, Adatia I et al (2013) Updated clinical classification of pulmonary hypertension. *J Am Coll Cardiol* 62:D34–D41
- Tuder RM, Archer SL, Dorfmueller P et al (2013) Relevant issues in the pathology and pathobiology of pulmonary hypertension. *J Am Coll Cardiol* 62:D4–D12
- D'Alonzo GE, Barst RJ, Ayres SM et al (1991) Survival in patients with primary pulmonary hypertension. Results from a national prospective registry. *Ann Intern Med* 115:343–349
- Hoepfer MM, Lee SH, Voswinckel R et al (2006) Complications of right heart catheterization procedures in patients with pulmonary hypertension in experienced centers. *J Am Coll Cardiol* 48:2546–2552
- Swift AJ, Rajaram S, Hurdman J et al (2013) Noninvasive estimation of PA pressure, flow, and resistance with CMR imaging: derivation and prospective validation study from the ASPIRE registry. *JACC Cardiovasc Imaging* 6:1036–1047
- Hammerstingl C, Schueler R, Bors L et al (2012) Diagnostic value of echocardiography in the diagnosis of pulmonary hypertension. *PLoS One* 7:e38519
- Nowak J, Hudzik B, Jastrzebski D et al (2018) Pulmonary hypertension in advanced lung diseases: echocardiography as an important part of patient evaluation for lung transplantation. *Clin Respir J* 12:930–938
- Johns CS, Rajaram S, Capener DA et al (2018) Non-invasive methods for estimating mPAP in COPD using cardiovascular magnetic resonance imaging. *Eur Radiol* 28:1438–1448
- Fisher MR, Forfia PR, Chamera E et al (2009) Accuracy of Doppler echocardiography in the hemodynamic assessment of pulmonary hypertension. *Am J Respir Crit Care Med* 179:615–621
- Kuriyama K, Gamsu G, Stern RG, Cann CE, Herfkens RJ, Brundage BH (1984) CT-determined pulmonary artery diameters in predicting pulmonary hypertension. *Invest Radiol* 19:16–22
- Corson N, Armato SG, Labby ZE, Straus C, Starkey A, Gombert-Maitland M (2014) CT-based pulmonary artery measurements for the assessment of pulmonary hypertension. *Acad Radiol* 21:523–530
- Ley S, Kreitner K-F, Fink C, Heussel CP, Borst MM, Kauczor H-U (2004) Assessment of pulmonary hypertension by CT and MR imaging. *Eur Radiol* 14:359–368
- Gerges M, Gerges C, Lang IM (2015) Advanced imaging tools rather than hemodynamics should be the primary approach for diagnosing, following, and managing pulmonary arterial hypertension. *Can J Cardiol* 31:521–528
- Pérez-Enguix D, Morales P, Tomás JM, Vera F, Lloret RM (2007) Computed tomographic screening of pulmonary arterial hypertension in candidates for lung transplantation. *Transplant Proc* 39:2405–2408
- Shen Y, Wan C, Tian P et al (2014) CT-base pulmonary artery measurement in the detection of pulmonary hypertension: a meta-analysis and systematic review. *Medicine (Baltimore)* 93:e256
- Rengier F, Wörz S, Melzig C et al (2016) Automated 3D volumetry of the pulmonary arteries based on magnetic resonance angiography has potential for predicting pulmonary hypertension. *PLoS One* 11:e0162516
- Froelich JJ, Koenig H, Knaak L, Krass S, Klose KJ (2008) Relationship between pulmonary artery volumes at computed tomography and pulmonary artery pressures in patients with- and without pulmonary hypertension. *Eur J Radiol* 67:466–471
- Linguraru MG, Pura JA, Gladwin MT et al (2014) Computed tomography correlates with cardiopulmonary hemodynamics in pulmonary hypertension in adults with sickle cell disease. *Pulm Circ* 4:319–329
- Linguraru MG, Pura JA, Van Uiter RL et al (2010) Segmentation and quantification of pulmonary artery for noninvasive CT assessment of sickle cell secondary pulmonary hypertension. *Med Phys* 37:1522
- Colin GC, Gerber BL, de Meester de Ravenstein C et al (2018) Pulmonary hypertension due to left heart disease: diagnostic and prognostic value of CT in chronic systolic heart failure. *Eur Radiol* 62:D34–D11
- Du Bois D, Du Bois EF (1916) A formula to estimate the approximate surface area if height and weight be known. *Arch Intern Med* 17:863–871
- Sciomer S, Magri D, Badagliacca R (2007) Non-invasive assessment of pulmonary hypertension: Doppler-echocardiography. *Pulm Pharmacol Ther* 20:135–140
- Pepi M, Tamborini G, Galli C et al (1994) A new formula for echo-Doppler estimation of right ventricular systolic pressure. *J Am Soc Echocardiogr* 7:20–26
- Biesdorf A, Rohr K, Feng D et al (2012) Segmentation and quantification of the aortic arch using joint 3D model-based segmentation and elastic image registration. *Med Image Anal* 16:1187–1201
- Wörz S, Rohr K (2007) Segmentation and quantification of human vessels using a 3-D cylindrical intensity model. *IEEE Trans Image Process* 16:1994–2004
- Wörz S, von Tengg-Kobligh H, Henninger V et al (2010) 3-D quantification of the aortic arch morphology in 3-D CTA data for endovascular aortic repair. *IEEE Trans Biomed Eng* 57:2359–2368
- Truong QA, Massaro JM, Rogers IS et al (2012) Reference values for normal pulmonary artery dimensions by noncontrast cardiac computed tomography: the Framingham heart study. *Circ Cardiovasc Imaging* 5:147–154
- Bujang MA, Adnan TH (2016) Requirements for minimum sample size for sensitivity and specificity analysis. *J Clin Diagn Res* 10:YE01–YE06
- Li J, Fine J (2004) On sample size for sensitivity and specificity in prospective diagnostic accuracy studies. *Stat Med* 23:2537–2550
- Tan RT, Kuzo R, Goodman LR, Siegel R, Haasler GR (1998) Utility of CT scan evaluation for predicting pulmonary hypertension in patients with parenchymal lung disease. *Chest* 113:1250–1256
- Ng CS, Wells AU, Padley SPG (1999) A CT sign of chronic pulmonary arterial hypertension: the ratio of main pulmonary artery to aortic diameter. *J Thorac Imaging* 14:270–278
- Kauffmann C, Tang A, Therasse É et al (2012) Measurements and detection of abdominal aortic aneurysm growth: accuracy and reproducibility of a segmentation software. *Eur J Radiol* 81:1688–1694
- Kontopodis N, Metaxa E, Papaharilaou Y, Georgakarakos E, Tsetis D, Ioannou CV (2014) Value of volume measurements in evaluating abdominal aortic aneurysms growth rate and need for surgical treatment. *Eur J Radiol* 83:1051–1056
- Devaraj A, Wells AU, Meister MG, Corte TJ, Wort SJ, Hansell DM (2010) Detection of pulmonary hypertension with multidetector CT and echocardiography alone and in combination. *Radiology* 254:609–616

36. Devaraj A, Loveridge R, Bosanac D et al (2014) Portopulmonary hypertension: improved detection using CT and echocardiography in combination. *Eur Radiol* 24:2385–2393
37. Rajani RR, Johnson LS, Brewer BL et al (2014) Anatomic characteristics of aortic transection: centerline analysis to facilitate graft selection. *Ann Vasc Surg* 28:433–436
38. Rengier F, Weber TF, Giesel FL, Böckler D, Kauczor H-U, von Tengg-Kobligh H (2009) Centerline analysis of aortic CT angiographic examinations: benefits and limitations. *AJR Am J Roentgenol* 192:W255–W263

**Publisher's note** Springer Nature remains neutral with regard to jurisdictional claims in published maps and institutional affiliations.

## Affiliations

Claudius Melzig<sup>1,2</sup> · Stefan Wörz<sup>3</sup> · Benjamin Egenlauf<sup>4</sup> · Sasan Partovi<sup>5</sup> · Karl Rohr<sup>3</sup> · Ekkehard Grünig<sup>2,4</sup> · Hans-Ulrich Kauczor<sup>1,2</sup> · Claus Peter Heussel<sup>1,2,6</sup> · Fabian Rengier<sup>1,2,7</sup> 

<sup>1</sup> Department of Diagnostic and Interventional Radiology, Heidelberg University Hospital, Im Neuenheimer Feld 110, 69120 Heidelberg, Germany

<sup>2</sup> Translational Lung Research Center Heidelberg (TLRC), Member of the German Center for Lung Research (DZL), University of Heidelberg, Heidelberg, Germany

<sup>3</sup> Biomedical Computer Vision Group, BIOQUANT, IPMB and German Cancer Research Center (DKFZ), University of Heidelberg, Heidelberg, Germany

<sup>4</sup> Centre for Pulmonary Hypertension, Thoraxklinik at Heidelberg University Hospital, Heidelberg, Germany

<sup>5</sup> Department of Radiology, Section of Interventional Radiology, Cleveland Clinic Foundation, Cleveland, OH, USA

<sup>6</sup> Department of Radiology, Thoraxklinik at Heidelberg University Hospital, Heidelberg, Germany

<sup>7</sup> Department of Radiology, German Cancer Research Center (DKFZ), Heidelberg, Germany